

Native osmium from the Guli Massif, Northern Siberia, Russia

Roland K. W. Merkle¹, Kreshimir Nenadovitch Malitch^{2,3,*}, Peter P. H. Gräser¹ and Inna Yu. Badanina³

¹Applied Mineralogy Group, Department of Earth Sciences, University of Pretoria, Pretoria, South Africa

²Department of Geochemistry and Ore-Forming Processes, A.N. Zavaritsky Institute of Geology and Geochemistry, the Uralian Branch of Russian Academy of Sciences, Ekaterinburg, Russia

³Department of Geochemistry, A.P. Karpinsky Russian Geological Research Institute, St. Petersburg, Russia

*Correspondence to: dunit2009@rambler.ru

Summary

Native osmium from two different placer occurrences (i.e., Ingarinda and Burlakovsky) within the Guli Massif, Maimecha-Kotui Province, was evaluated for mineral compositions that show systematic differences between the localities. Grains of native osmium show increases in iridium towards the rim, and nuggets consisting of aggregates define trends of preferential substitution of osmium by iridium. A statistically reliable difference in Os/Ir ratios between the two studied placers can be demonstrated. From textural and compositional characteristics it is concluded that the native osmium of the Burlakovsky placer formed at temperatures higher than can be assumed to be reasonable for crustal conditions. The difference in the Os/Ir ratios between the two placers can be attributed to fractional crystallization of native osmium either in the mantle source, which was tapped in different events to form the Guli Massif, or to decreasing Os/Ir values during crystallization under crustal conditions after intrusion of the silicate melt(s).

Introduction

According to the presently accepted nomenclature (Harris and Cabri 1991), the Os-rich alloys in the placers of the Guli Massif (Balmasova et al. 1992; Malitch and Lopatin 1997b; Malitch et al. 2002) are to be called osmium. To avoid confusion with osmium as an element, we will refer to the mineral grains as native osmium.

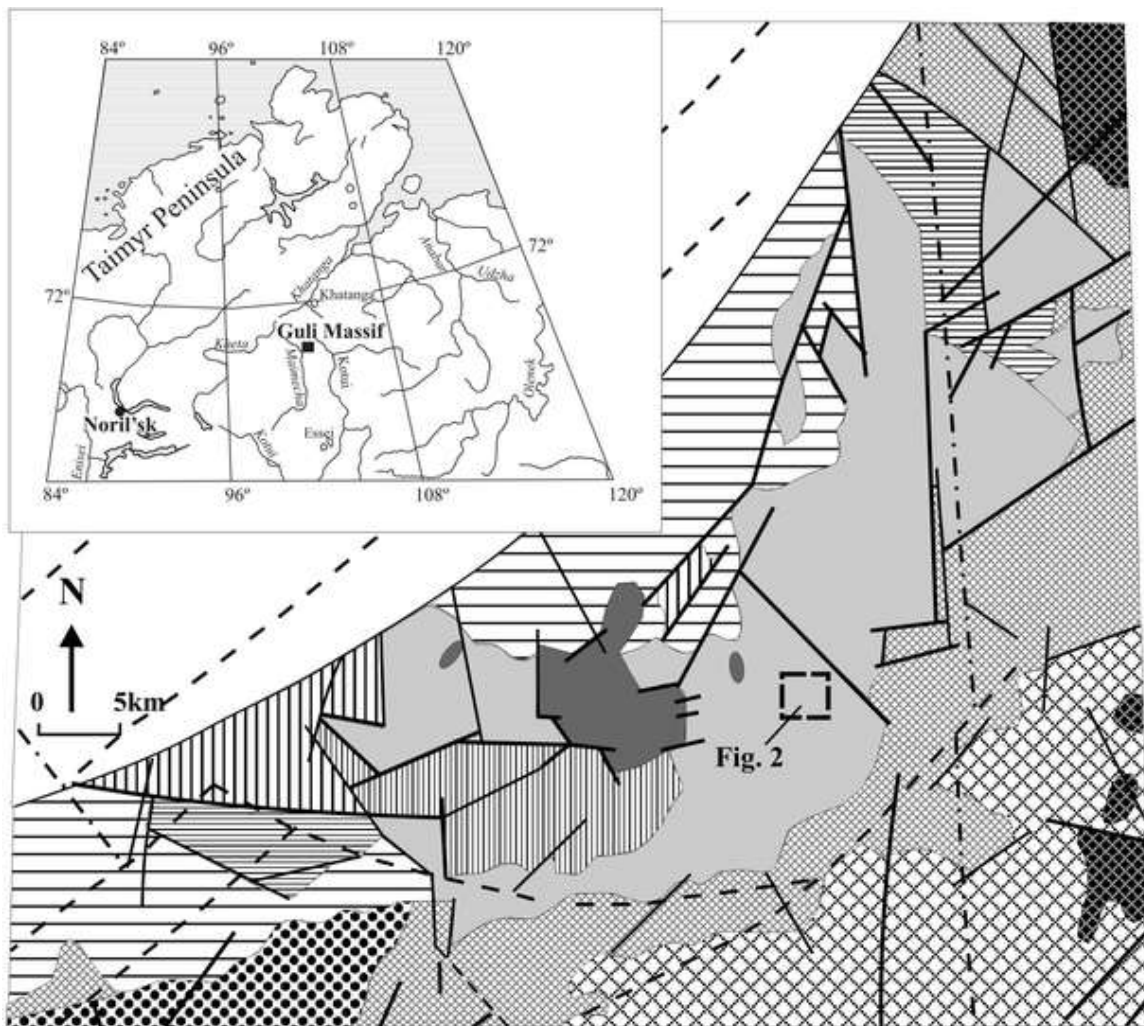
Native osmium has been described in situ from ophiolites (Dmitrenko et al. 1985; Legendre and Augé 1986; Augé and Johan 1988; Ohnenstetter et al. 1991; Ohnenstetter 1992; Melcher et al. 1997; Augé et al. 1998; Garuti et al. 1999; Melcher 2000; Zaccarini et al. 2005; Ahmed 2007; Shi et al. 2007; El Ghorfi et al. 2008; Kapsiotis et al. 2009; Uysal et al. 2009; Gonzalez-Jimenez et al. 2010 and references cited therein) layered intrusions (Cabri and Laflamme 1988; Balabonin et al. 1994; Merkle 1998), and predominantly from placer deposits all over the world (Feather 1976; Cabri et al. 1996; Malitch 1996; Krstić and Tarkian 1997; Nakagawa and Franko 1997; Gornostayev et al. 1999; Weiser and Bachmann 1999;

Weiser 2002; Malitch and Merkle 2004; Barkov et al. 2005; Tolstykh et al. 2005, 2009 among many others). For many placers, the location and type of the source rocks (e.g. an ophiolite) of the osmium-rich alloy grains is completely unknown. In other cases, the petrological characteristics of the source rocks are unknown, even if the placers can be attributed to a known geological body. In all the placers, the native osmium can either be found as single grains or, predominantly, as lamellae and inclusions in grains of Pt-Fe alloys (Cabri et al. 1996). Obviously, the textural differences and assemblages imply distinct particularities during formation.

Huge databases of microprobe analyses of osmium-rich Os-Ir-Ru(\pm Pt \pm Rh) alloys are available in the literature (Feather 1976; Dmitrenko et al. 1985; Cabri et al. 1996; Cabri 2002) and allow delineation of broad compositional trends. Unfortunately, these databases are not conducive to an evaluation of the genetic reasons behind the chemical variations observed in these minerals. Most native osmium is found in placers (like in the Witwatersrand basin) which derived their material from a large and, in all probability, geologically complex source area (Cousins 1973; Merkle and Franklin 1999; Malitch and Merkle 2004, among others). Consequently, a large scatter of compositional variation is observed. For instance, the Os-Ir-Ru alloys from the Evander Goldfield, located at the eastern extremity of the Witwatersrand Basin (see Fig. 1 in Malitch and Merkle 2004), differs from those of the other six goldfields (i.e., East Rand, Central Rand, West Rand, Carletonville, Klerskorp, and Welcom) in systematically higher Ru contents and different modal proportions of chemically distinct Os-rich alloys. Detailed evaluations of compositional trends of native osmium from a lithologically homogeneous source, that could facilitate the establishment of correlation between systematic substitutions and petrological evolution of the source rocks, are missing.

The Guli Massif in northern Siberia, Russia (Zhabin 1965; Butakova 1974; Vasil'ev and Zolotukhin 1975; Egorov 1991; Malitch 1999) contains one of the world's largest resources of osmium metal in numerous river placers (Malitch et al. 1996, 1998, 2002; Malitch and Lopatin 1997b). Owing to the large size of the Guli Massif, and the consistency of relatively restricted range of lithological units over large distances, the Quaternary sediments of numerous rivers in the area can have obtained osmium-rich alloy grains only from a limited variation of rock types in the source area. This affords the opportunity for a systematic investigation of compositional variations of Os-Ir-Ru alloys from individual river placers within the Guli Massif and to compare differences between placers that are due to differences in the source area.

Here we report on the chemical composition of Os-rich alloy grains, which were sampled during prospecting in the area of the Ingaringda river in the southern part of the Guli Massif (Fig. 1).





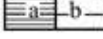







-  Terrigenous sediments (J₃-K₁) of Khatanga trough
-  Picrite - meimechite complex (T_{1,2}), meimechite and picrite porphyrites:
(a) Maimechian suite, (b) subvolcanic and dike facies
-  Delkanian suite (T₁): (a) trachybasalts and andesites, (b) augites, limburgites, and nephelinites
-  Tyvankitian suite (T₁): trachybasalts and trachyandesite-basalts
-  Kogotokian suite (T₁): basalts
-  Arydzhangian suite (P₂-T₁): alkaline picrites, foidites, and alkaline leucobasalts
-  Pravoboyarian suite (P₂-T₁): basic pyroclastic rocks
-  Ijolite-carbonatite complex(T₁): alkaline-ultrabasic and alkaline rocks, and carbonatites
-  Clinopyroxenite-dunite complex (D₃-C₁): dunites, chromitites, and clinopyroxenites
-  Faults: (a) Enisei-Kotui system separating super-large structures, (b) Sayano-Anabar system, separating large blocks of the platform, (c) in the basement that act as magma conduits, and (d) within the platform cover

Fig. 1. Map of the Guli Massif and the location of the sampling area

Geological background and sample location

The Guli ultramafic complex, located in the Maimecha-Kotui Province (Vasil'ev and Zolotukhin 1995) in northern part of Siberian Craton, is remarkable for its considerable size. It is controlled by the Taimyr-Baikal and Enisei-Kotui paleorift structures (Malitch 1999). The complex covers an area of 600 km² but geophysical evidence shows that it extends for a total of 2,000 km² (Egorov 1991) and is thus the world's largest clinopyroxenite-dunite massif (Malitch and Lopatin 1997a). Dunite (Fo₈₅₋₉₃) predominates, forming a crescent-shaped, plate-like body 30 km long and 10 to 15 km wide covering an area of approximately 450 km², dipping 15° to 20° to the northwest (Fig. 1). Vein-type bodies of chromitite are abundant at the periphery of the southern part of the massif. Wehrlite and magnetite-rich clinopyroxenite form dikes, stockworks, and lenticular bodies within the dunite. A restricted number of bedrock-hosted platinum-group minerals (PGM) in dunite and chromitite have been described by Balmasova et al. (1992); Malitch and Rudashevsky (1994); Malitch (1999) and Malitch et al. (2003, 2005, 2011).

To the southwest, the clinopyroxenite-dunite complex is overlain by the picrite-meimechite complex, composed of ultramafic rocks (known as meimechites) of the Maimechian volcanic suite and subvolcanic lithologies (Malitch and Lopatin 1997a; Sobolev et al. 2009), whereas in its central part stock-like bodies of a 220–240 Ma ijolite-carbonatite complex (Fig. 1), occupying an area of less than 35 km² (Egorov 1991; Kogarko et al. 1995 and references cited therein), are present.

Compared to other clinopyroxenite-dunite complexes the Guli ultramafic massif is characterized by its atypical size (with an exposed area of about 450 km²) with most other complexes being much smaller in size, e.g. ~ 60 km² for Tulameen (St. Louis et al. 1986), ~ 45 km² for Nizhny Tagil (Betekhtin 1961; Efimov 1998), ~60 km² for Kondyor (Rozhkov et al. 1962; Burg et al. 2009) or ~20 km² for Inagli (Rozhkov et al. 1962; Mues-Schumacher et al. 1996). The ultramafic rock assemblage of the Guli Massif and its significant potential for placer PGM accumulations make it typical of zoned massifs of the Uralian-Alaskan-Aldan type, whereas the huge size of the ultramafic complex, its shape, the lack of concentrically zoned structure, and the common occurrence of refractory Ir-, Os-, and Ru-rich PGM in chromitite and placer deposits are features more consistent to those of ophiolite massifs. It thus exhibits transitional features between typical zoned platiniferous clinopyroxenite-dunite and ophiolitic dunite-harzburgite complexes.

The age of the Guli complex remains a subject of controversy. A recent Pb isotope investigation by Kogarko and Zartman (2007) suggested an age of 251 ± 11 Ma for the entire complex, similar to that previously obtained by ⁴⁰Ar/³⁹Ar study (Egorov 1991). This is in marked contrast with a mean ¹⁸⁷Os/¹⁸⁸Os age obtained from Os-rich alloys derived from dunite (370 ± 40 Ma, Malitch and Kostoyanov 1999) and a Re-Os isochron age for dunite (329 ± 57 Ma, McKelson et al. 2005), both of which support the hypothesis of Zhabin (1965) that the dunite may be much older than other rocks of the Guli area. Finally, Dalrymple et al. (1995) obtained a ⁴⁰Ar/³⁹Ar age of 436 ± 2 Ma for biotite from carbonatite of the ijolite-carbonatite complex, while U-Pb age of baddeleyite from carbonatite gave a weighted mean of 310.4 ± 2.8 Ma (MSWD = 0.61, probability 0.86; *n* = 15, LA MC-ICP-MS, Macquarie University, Australia; unpublished data of K.N. Malitch and E.A. Belousova).

Sixteen grains of Os-rich alloys were obtained from Quaternary sediments of the Ingaringda River (i.e., prospecting line L-365), and nine grains from the Quaternary sediments of the Burlakovskiy Creek (prospecting line L-2), the left tributary of the Ingaringda River (Fig. 2). It is noteworthy that dunite is the only rock exposed in the catchment area of the Burlakovskiy stream, while different rock-lithologies (e.g., dunite, chromitite and clinopyroxenite) can be observed in the catchment area of the Ingaringda River. This implies that Os-rich grains of different compositions may have been derived from distinct rock sources.

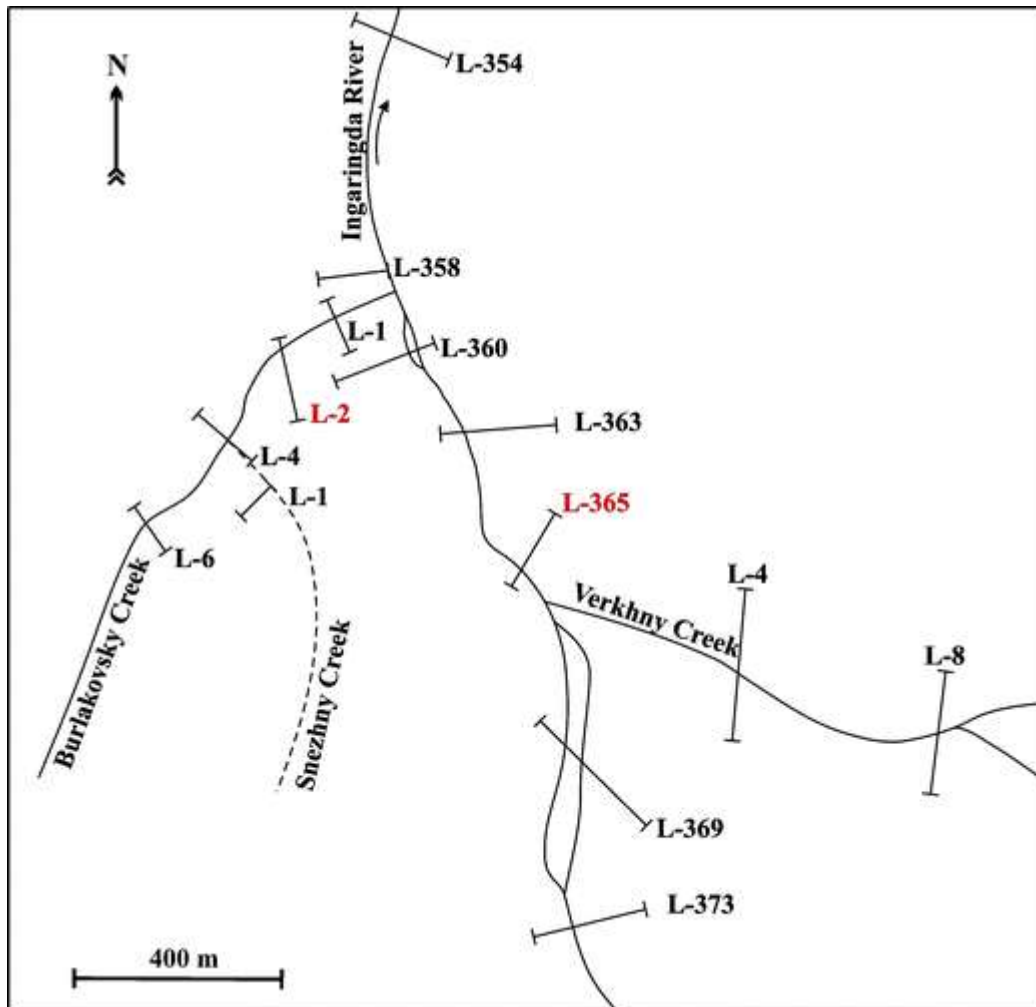


Fig. 2. Location of the Os-rich grains at Ingaringda (prospecting line L-365) and Burlakovskiy (prospecting line L-2)

The granulometry of the PGM nuggets at Ingaringda and Burlakovskiy is determined by five size classes (in mm): 0.25–0.5 (56 and 63%, respectively), 0.125–0.25 (33 and 29%), 0.5–1.0 (9 and 7%), >1 (about 1 and 0%), <0.125 (around 1% each), implying that the size range 0.25–0.5 mm dominates the PGM budget of placer deposits. The osmium grains analysed in this study are nuggets (crystals and aggregates) of the most abundant size fraction - 0.5 + 0.25 mm.

Analytical conditions

Analyses were carried out with a Jeol 733 electron microprobe with attached Oxford ISIS (energy dispersive) system at the University of Pretoria. The accelerating potential and beam current were 20 kV and 20 nA, respectively, with acquisition times of 100 s per spot analysis. Spectra were recorded with the highest possible resolution for the pulse processing setting, referenced against Co, and processed for Os, Ir, Ru, Pd, Pt, Rh, Fe, Ni, and Cu. All elements but Os, Ir, and Ru were found to be below the statistically reliable detection limits under the analytical conditions.

Although no comprehensive study of systematic compositional variations within the nuggets was carried out, analyses in the centre and rims were carried out for the grains from Ingarinda, and multiple analysis spots in the grains from Burlakovsky. We obtained 34 analyses from the 16 grains from Ingarinda, and 58 analyses of 9 grains from Burlakovsky

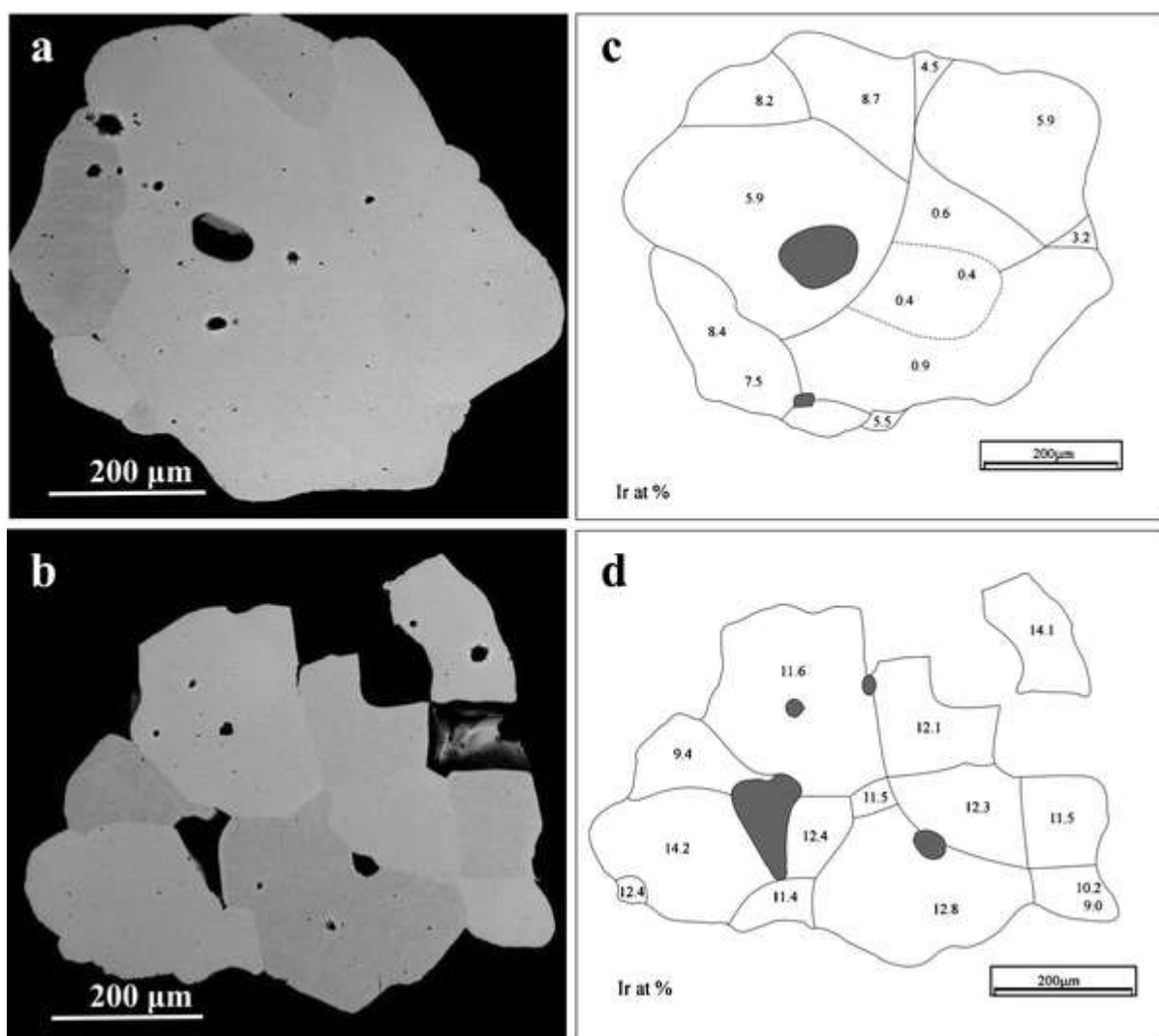


Fig. 3. Images of different aggregate nuggets from Burlakovsky (representing trends in Fig. 7). Back-scattered electron images (a and c), line drawings (b and d). Silicate inclusions (in black) are olivine and clinopyroxene

Results

Reflected light observations

Reflected light microscopic investigation of the 16 nuggets from Ingaringda revealed that 4 are aggregates composed of 2 to 4 visible grains, while among the 9 nuggets from Burlakovsky, 5 are aggregates with up to 13 sub-grains.

Figure 3 represent line drawings reproduced from backscatter images of two aggregates from Burlakovsky. The numbers give the determined Ir contents (in at.%) and represent the position of analyses. Microprobe analyses show that the largest variation between different sub-grains is due to Ir. Table 1 gives representative analyses. The mineralogical investigation shows that

Table 1. Selected electron microprobe analyses of Os-rich alloys from the Guli Massif

| Ru, wt% | Os, wt% | Ir, wt% | Total | Ru, at% | Os, at% | Ir, at% | Trend | Group |
|-------------|---------|---------|--------|---------|---------|---------|---------|-------|
| Burlakovsky | | | | | | | | |
| 0.32 | 100.29 | 0.66 | 101.27 | 0.59 | 98.76 | 0.64 | Trend 1 | BuG7 |
| 0.78 | 97.57 | 3.28 | 101.63 | 1.44 | 95.38 | 3.18 | Trend 1 | BuG7 |
| 0.24 | 101.19 | 0.45 | 101.88 | 0.44 | 99.13 | 0.44 | Trend 1 | BuG7 |
| 2.29 | 89.79 | 9.20 | 101.28 | 4.17 | 87.01 | 8.82 | Trend 1 | BuG7 |
| 1.47 | 92.82 | 6.04 | 100.33 | 2.72 | 91.40 | 5.89 | Trend 1 | BuG7 |
| 1.81 | 90.31 | 8.45 | 100.57 | 3.34 | 88.47 | 8.19 | Trend 1 | BuG7 |
| 2.07 | 89.77 | 9.05 | 100.89 | 3.80 | 87.48 | 8.73 | Trend 1 | BuG7 |
| 1.29 | 94.43 | 4.57 | 100.29 | 2.39 | 93.15 | 4.46 | Trend 1 | BuG7 |
| 1.55 | 92.36 | 6.02 | 99.93 | 2.87 | 91.24 | 5.88 | Trend 1 | BuG7 |
| 0.33 | 98.73 | 0.94 | 100.00 | 0.61 | 98.46 | 0.93 | Trend 1 | BuG7 |
| 1.72 | 91.03 | 7.76 | 100.51 | 3.17 | 89.29 | 7.53 | Trend 1 | BuG7 |
| 2.01 | 87.14 | 8.45 | 97.60 | 3.82 | 87.77 | 8.42 | Trend 1 | BuG7 |
| 2.10 | 89.83 | 8.77 | 100.70 | 3.85 | 87.68 | 8.47 | Trend 1 | BuG7 |
| 1.34 | 91.47 | 5.50 | 98.31 | 2.55 | 91.98 | 5.47 | Trend 1 | BuG7 |
| 1.08 | 94.15 | 4.60 | 99.83 | 2.02 | 93.45 | 4.52 | Trend 2 | BuG6 |
| 0.88 | 94.35 | 4.59 | 99.82 | 1.65 | 93.83 | 4.52 | Trend 2 | BuG6 |
| 2.44 | 84.06 | 14.89 | 101.39 | 4.44 | 81.30 | 14.26 | Trend 3 | BuG8 |
| 2.30 | 83.86 | 15.05 | 101.21 | 4.20 | 81.35 | 14.45 | Trend 3 | BuG8 |
| 2.15 | 82.72 | 14.51 | 99.38 | 4.01 | 81.79 | 14.20 | Trend 3 | BuG8 |
| 2.11 | 83.04 | 14.35 | 99.50 | 3.92 | 82.05 | 14.03 | Trend 3 | BuG8 |
| 0.36 | 94.65 | 5.08 | 100.09 | 0.68 | 94.31 | 5.01 | Trend 4 | BuG1 |
| 0.24 | 94.02 | 6.70 | 100.96 | 0.45 | 92.99 | 6.56 | Trend 4 | BuG1 |
| 0.12 | 83.90 | 16.60 | 100.62 | 0.23 | 83.44 | 16.33 | Trend 5 | BuG4 |
| 0.29 | 88.74 | 12.15 | 101.18 | 0.54 | 87.59 | 11.86 | Trend 5 | BuG4 |
| 0.53 | 82.69 | 17.63 | 100.85 | 0.98 | 81.77 | 17.25 | Trend 5 | BuG4 |
| Ingaringda | | | | | | | | |
| 3.41 | 80.66 | 15.70 | 99.77 | 6.26 | 78.61 | 15.14 | G1 core | G1 |
| 3.26 | 80.68 | 15.58 | 99.52 | 6.01 | 78.91 | 15.08 | G1 rim | G1 |

| Ru, wt% | Os, wt% | Ir, wt% | Total | Ru, at% | Os, at% | Ir, at% | Trend | Group |
|---------|---------|---------|--------|---------|---------|---------|----------|-------|
| 3.32 | 77.95 | 19.34 | 100.61 | 6.04 | 75.44 | 18.53 | G2 core | G2 |
| 3.85 | 75.46 | 21.49 | 100.80 | 6.97 | 72.58 | 20.45 | G2 rim | G2 |
| 2.47 | 85.64 | 13.03 | 101.14 | 4.50 | 83.00 | 12.49 | | G3 |
| 2.46 | 84.84 | 13.43 | 100.73 | 4.51 | 82.56 | 12.93 | | G3 |
| 2.47 | 85.63 | 12.25 | 100.35 | 4.54 | 83.62 | 11.84 | G4 core | G4 |
| 2.63 | 86.71 | 12.83 | 102.17 | 4.74 | 83.09 | 12.16 | G4 rim | G4 |
| 2.01 | 88.12 | 11.88 | 102.01 | 3.65 | 85.01 | 11.34 | | N1 |
| 2.33 | 85.43 | 14.57 | 102.33 | 4.20 | 81.96 | 13.84 | | N1 |
| 2.19 | 86.29 | 12.11 | 100.59 | 4.03 | 84.27 | 11.70 | | N1 |
| 3.12 | 81.84 | 17.93 | 102.89 | 5.57 | 77.61 | 16.83 | G5 core | G5 |
| 2.89 | 81.28 | 18.40 | 102.57 | 5.18 | 77.46 | 17.35 | G5 rim | G5 |
| 2.58 | 88.57 | 9.62 | 100.77 | 4.71 | 86.04 | 9.25 | | G6 |
| 2.02 | 91.45 | 7.93 | 101.40 | 3.68 | 88.71 | 7.61 | | G6 |
| 3.60 | 68.44 | 29.65 | 101.69 | 6.49 | 65.45 | 28.06 | | G7 |
| 3.46 | 69.96 | 29.53 | 102.95 | 6.16 | 66.19 | 27.65 | | G7 |
| 3.82 | 80.93 | 13.17 | 97.92 | 7.10 | 80.01 | 12.88 | G8 core | G8 |
| 1.71 | 83.52 | 12.75 | 97.98 | 3.24 | 84.06 | 12.70 | G8 rim | G8 |
| 2.69 | 82.71 | 14.06 | 99.46 | 4.98 | 81.33 | 13.68 | | N2 |
| 2.91 | 81.87 | 13.37 | 98.15 | 5.44 | 81.41 | 13.15 | | N2 |
| 2.86 | 82.55 | 14.19 | 99.60 | 5.27 | 80.95 | 13.77 | | N3 |
| 2.99 | 81.19 | 14.81 | 98.99 | 5.54 | 80.02 | 14.44 | | N3 |
| 4.28 | 61.54 | 32.83 | 98.65 | 7.88 | 60.29 | 31.83 | | G9 |
| 3.92 | 62.47 | 34.27 | 100.66 | 7.11 | 60.21 | 32.68 | | G9 |
| 3.64 | 73.31 | 21.73 | 98.68 | 6.73 | 72.11 | 21.16 | | N4 |
| 4.11 | 73.05 | 23.34 | 100.50 | 7.44 | 70.32 | 22.24 | | N4 |
| 3.70 | 73.27 | 20.67 | 97.64 | 6.92 | 72.76 | 20.31 | | N4 |
| 3.72 | 72.58 | 22.45 | 98.75 | 6.87 | 71.31 | 21.82 | G10 core | G10 |
| 3.63 | 72.29 | 23.61 | 99.53 | 6.67 | 70.53 | 22.80 | G10 rim | G10 |
| 3.63 | 74.78 | 21.86 | 100.27 | 6.61 | 72.43 | 20.95 | | G11 |
| 3.87 | 73.67 | 21.04 | 98.58 | 7.16 | 72.38 | 20.46 | | G11 |
| 3.57 | 76.17 | 19.86 | 99.60 | 6.56 | 74.28 | 19.17 | | G12 |
| 3.43 | 74.77 | 18.59 | 96.79 | 6.48 | 75.05 | 18.46 | | G12 |

Lower level of detection was ~0.03 wt.%

Trends refer to numbered trends in Fig. 7

- aggregates are mosaics of euhedral and partly unhedral sub-grains;
- sub-grains show only small compositional heterogeneities;
- boundaries between sub-grains are sharp and smooth, with little to no obvious indications for compositional adjustments during agglomeration;
- sub-grain sharing edges can differ by several atomic percent in their Ir content, while their Ru contents typically vary much less;
- the range of Ir contents differ between different aggregates;

- there is no systematic geometric arrangement of sub-grains in aggregates which would allow recognition of an evolutionary compositional trend based on core-rim variations;
- inclusions consist of very complex mixture of silicates, oxides, and sulphides.

Compositional variations

Figure 4 shows the chemical variation encountered in this study. All grains plot in the Os field and thus are native Os, with significant Os - Ir substitution (Fig. 5) and a lesser amount of Ru for Os (\pm Ir). Some overlap exists, but the grains from Ingarinda display a larger range of Os/Ir ratios at higher Ir contents than the grains from Burlakovsky.

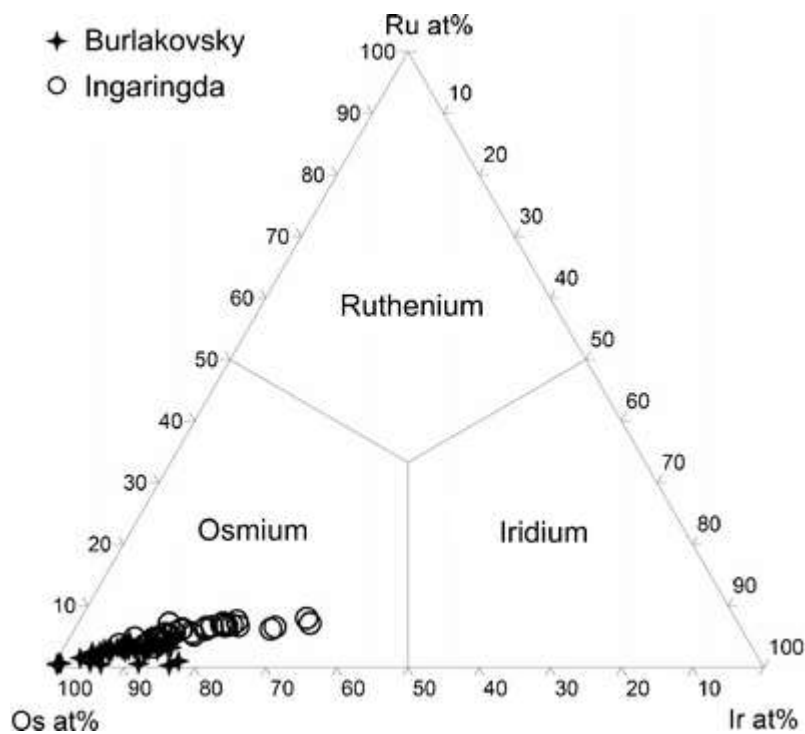


Fig. 4. Compositional variation of Os-rich alloys (in atomic proportions) from this study

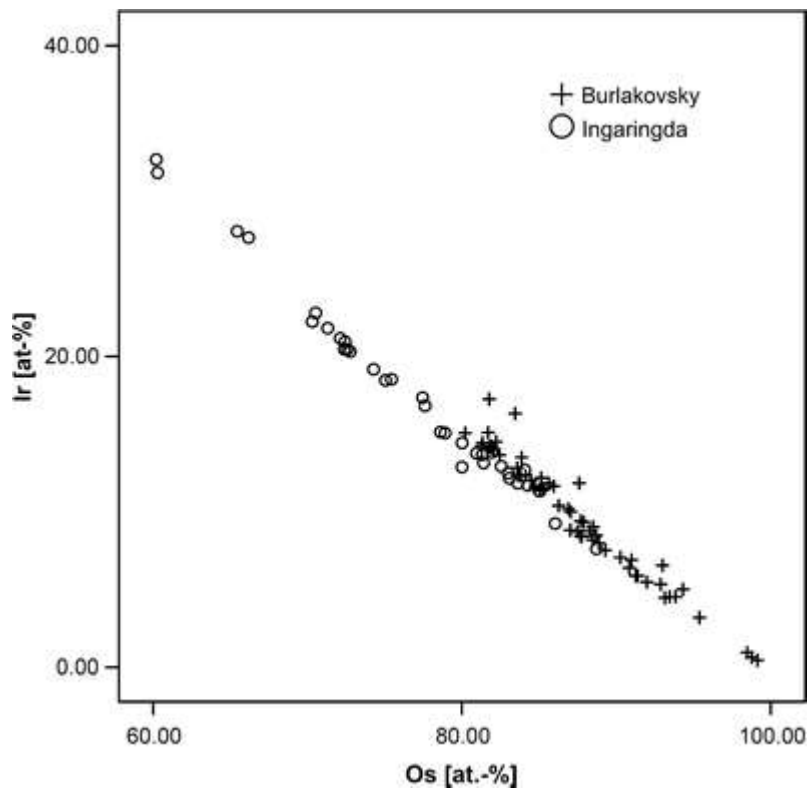


Fig. 5. Relationship between Os and Ir in native osmium from the Guli Massif. The small amounts of scatter are due to Ru contents (see Fig. 6). There is a significant difference in the average Os/Ir ratio of the two localities

The ratio between Ru and Ir is rather variable (Fig. 6), with most analyses from Ingaringda implying Ir/Ru values between 2 and ~4, with Ru contents of native osmium from Ingaringda being, on average, higher than those from Burlakovsky. Most of the trends defined by aggregates and grains from Burlakovsky show the same sense of change as defined by 15 analyses from one aggregate (trend 1 in Fig. 7), i.e., substitution of Os by Ir and Ru with an Ir/Ru ratio of 2.3. However, 1 grain (trend 2 in Fig. 7) and 4 analyses from 1 aggregate (trend 3 in Fig. 7) are characterised by slight variations in Ru by less than 0.5 at.% at almost constant Ir. Two additional grains from Burlakovsky do not follow the general trend and imply another trend of increasing Ir contents at constantly very low Ru contents (trends 4 and 5 in Fig. 7).

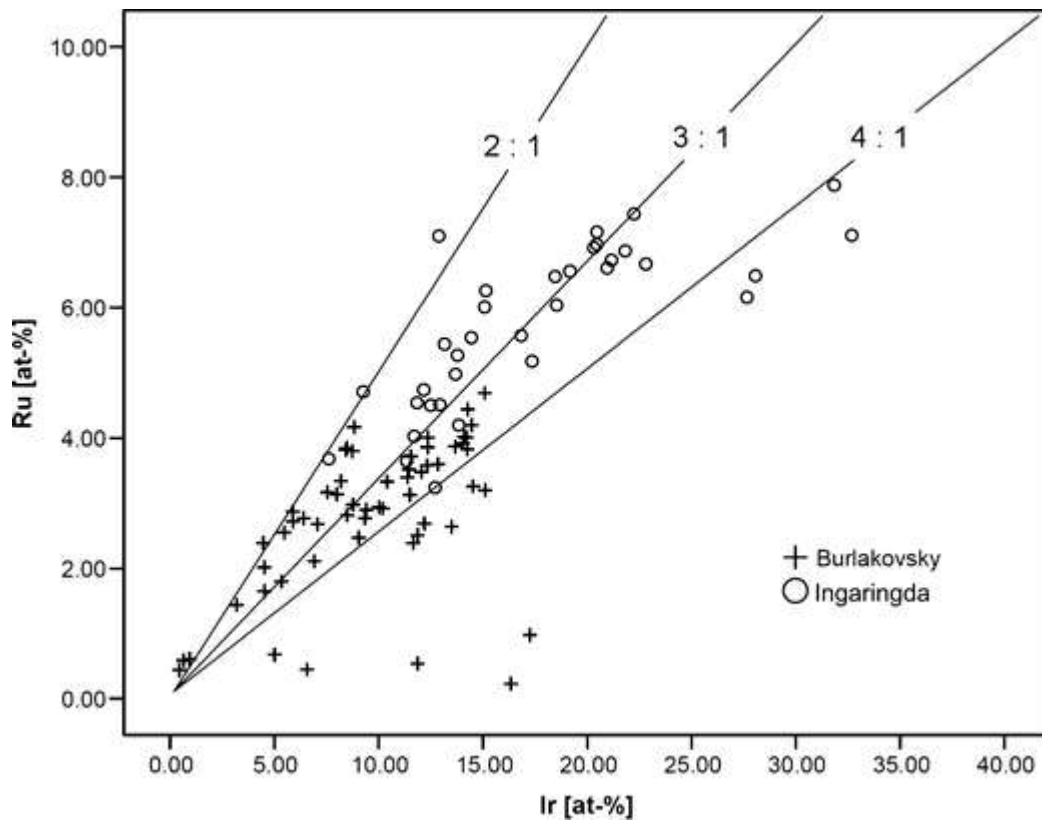


Fig. 6. Scatter in the relationship between Ru and Ir. Note the lower Ru contents in native osmium from Burlakovsky and the associated trend of increasing Ir at very low Ru

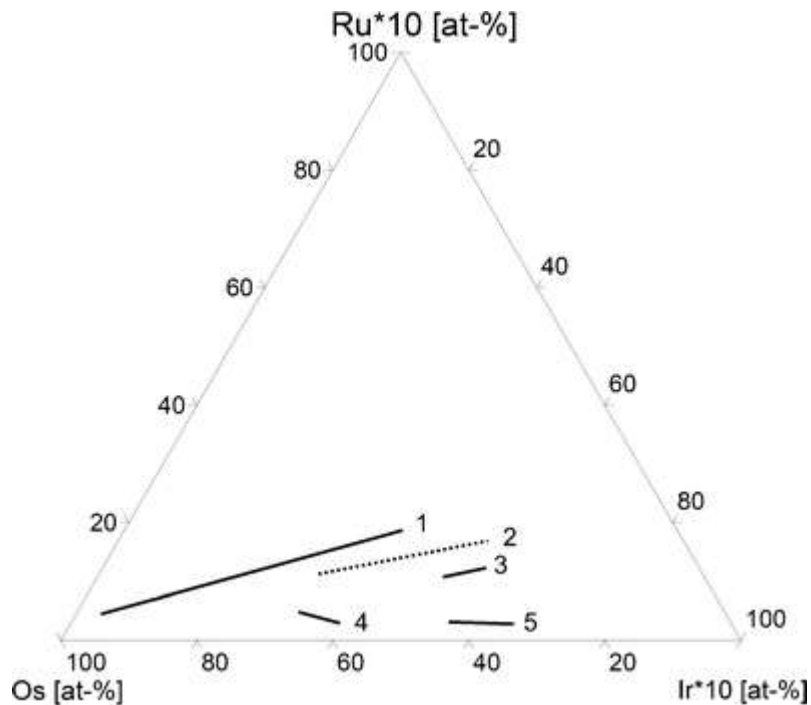


Fig. 7. Chemical variations in grains and aggregate nuggets from Burlakovsky. 1 = aggregate of 15 sub-grains; 2 = grain with variation in Ru; 3 = aggregate nugget with variation in Ru; 4, 5 = grains representing a trend of increasing Ir at very low Ru. See text for discussion

The chemical variation within the aggregates from Ingaringda is less pronounced than that in the aggregates from Burlakovsky, possibly because of the smaller number of sub-grains. Tests for compositional differences between the cores of grains and their rims showed a statistically reliable increase in Ir between centre and rim by up to 2 at.% Ir in five grains from Ingaringda, with Ru being constant within analytical uncertainty. Only one grain showed a pronounced drop in Ru-content (by 3.9 at.%) from core to rim (Fig. 8).

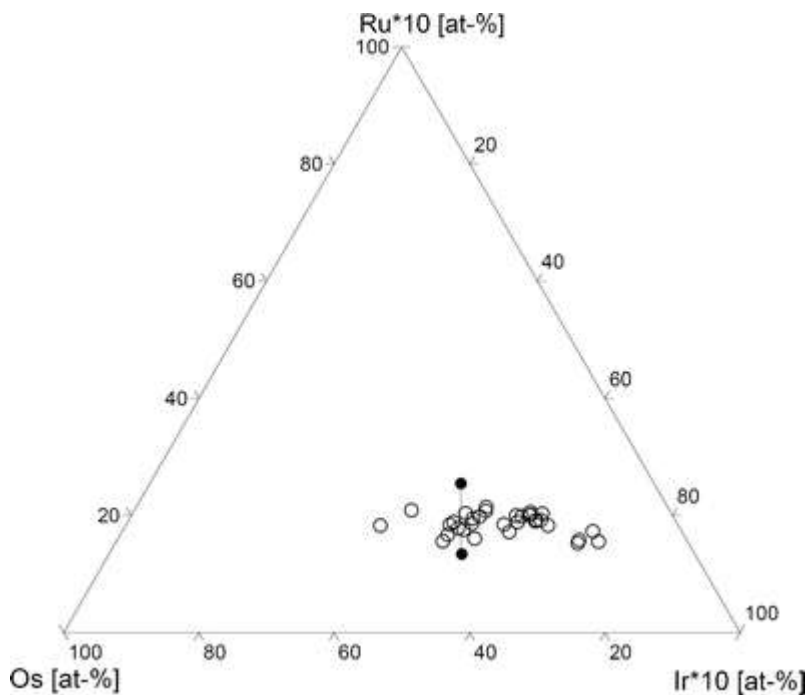


Fig. 8. Chemical compositions of native osmium from Ingaringda. The line represents variation between 2 analyses in one grain with a drop in Ru from core to rim

Discussion

Compositional heterogeneity of nuggets

Previous investigations of Os-rich alloys from Guli Massif emphasized the dominant role of native osmium among PGM nuggets in placer deposits (Balmasova et al. 1992; Malitch et al. 2002). No chemical zoning within PGM grains were formerly presented, whereas in this study small differences in some grains were observed. In all of these cases the rims are slightly enriched in Ir (up to 2 at.%).

Figure 3 shows the Ir-contents in two aggregate nuggets from Burlakovsky (see also Fig. 7). There is no obvious systematic in the distribution of Ir-contents in these nuggets which would permit an arrangement in chronological order of formation of the individual sub-grains. It is, however, obvious that grains are aggregated, which represent different stages of alloy formation. The sub-grains are easily discernible based on their optical orientation and composition within the nugget. Our microprobe study shows that there is very little, if any, chemical equilibration between the sub-grains, i.e. after formation.

The compositional variation implies that some fractionation of Os, Ir, and Ru occurred during the growth of the individual grains of native osmium. The compositional differences between sub-grains in some nuggets show that this could not have happened simultaneously. This implies that the reservoir from which they derived had not been homogeneous. This growth step must have been followed by an agglomeration process in which grains of native osmium, formed under varying conditions, were brought together and agglomerated.

To understand the chemical evolution of the native osmium, the crystallization paths and thermal stabilities in the system Os-Ir-Ru are unlikely to provide an answer. Equilibrium phase relations of Os-Ir (i.e., the binary system which approaches the composition of the investigated alloys), as well as Os-Ru and Ir-Ru suggest that these alloys have minimal thermal stabilities close to 2,800°C at surface pressure (Massalski 1993), which may be lowered only slightly by the presence of Ru. Such temperatures can only be reached close to the core—mantle boundary (Boehler 1996; Sherman 1997), an environment that has been proposed for other Os-rich alloys (Bird and Bassett 1980; Bird et al. 1999).

There are no experimental data to permit an evaluation of how Os-rich alloys behave in P-T-t space. Melts which may be the source for zoned complexes (Conrad and Kay 1984; Mues-Schumacher et al. 1996; Brüggemann et al. 1997) are unlikely to reach temperatures of even 1,400°C (Arculus 1994; Peacock et al. 1994; Schmidt and Poli 1998), and it is doubtful whether the degree of sintering as observed in the aggregates is possible at crustal pressures in a rapidly cooling volcanic system at less than half the crystallization temperature of the native osmium. It stands to reason that the textures of the agglomerated aggregates from Burlakovsky are easier to form under conditions of high temperature and high pressure. If it would be assumed that the Guli Massif represents an Uralian-Alaskan type intrusion, and if Uralian-Alaskan type intrusions are the product of arc volcanism (Murray 1972), then derivation of native osmium from the core—mantle boundary region becomes an unlikely scenario. On the other hand, if the Guli Massif is considered as Aldan-type complex, which may have a translithospheric mantle origin (e.g., Kondyor; Burg et al. 2009), these massifs could be well corresponded according to osmium isotope studies (Malitch 1998; Malitch and Kostoyanov 1999; Malitch et al. 2005, 2007, among others). These studies indicated a near-to-chondritic source with no obvious crustal contamination and are therefore in accordance with a deep mantle source of the native osmium.

Chemical zoning has often been frequently observed in Os-rich alloys (Hiemstra 1964; Koen 1964; Cousins 1973), but quantification of subtle chemical changes in metal ratios in Os-Ir-Ru alloys has not received much attention. A detailed study of zonation in such alloys (Cabri and Harris 1975) suggested that an increase of Ir towards the rim of nuggets can occur in some cases, but because of the much higher Ir content of the investigated alloys it is not clear if these findings are universally applicable. The observations in this study imply as well, that the evolutionary trend is from low to higher Ir content.

If the formation and derivation of native osmium grains from a deep mantle source are not accepted, then the availability of Os, Ir, and Ru in a magma during the direct crystallization from a melt are more likely to be the controlling mechanism for composition and zonation

(Peck et al. 1992). Then, however, it is also not possible to predict the resulting compositional trends if different types of magma are involved in the formation of the Guli Massif.

There is now irrefutable evidence that nuggets of Os-Ir-Ru alloys formed at high temperatures and that the observed chemical compositional variations represent primary features of the grains (Cabri and Harris 1975; Hattori and Cabri 1992; Peck et al. 1992; Bird et al. 1999; Okrugin 2002). This implies that the compositional evolution of alloy compositions must be related to the petrological evolution of the source rocks during Os-Ir-Ru alloys formation.

Trends in bulk composition

Previous studies of PGM from the Guli complex (Balmasova et al. 1992; Malitch and Lopatin 1997b; Malitch et al. 2002, 2003) contain graphical presentations of chemical features of Os-rich alloys, which are now supplemented with new analyses. The overall variation in Os-rich alloys observed in this study is smaller than the complete range encountered from placers in the Guli Massif to date. This is not surprising considering that this study focussed on a limited number of nuggets from limited areas within the Massif. That the investigated nuggets are of a specific size fraction is unlikely to have an effect on the results, because no relationship between size fraction and composition was observed (Balmasova et al. 1992). This is also implied by analyses of different size fractions of chromitite from the Guli Massif (Malitch and Rudashevsky 1994), where Os/Ir ratios vary within analytical uncertainty, although laurite (RuS_2) is another Os- and Ir-containing mineral present in chromitite (Malitch et al., 2003) and the placers of this complex (Malitch 1996 Malitch et al. 2002).

Taking into account the large number of microprobe analyses obtained, two distinct trends of compositional evolution within the alloys have been observed: a trend of Ir/Ru <1 at high contents of Os, and a replacement of Os by Ir at approximately constant Ru contents at slightly lower Os contents (Malitch and Lopatin 1997b; Malitch et al. 2002). These trends were not observed in the material studied here. Instead, there seems to be always a higher proportion of Ir than Ru substituting for Os, with even very low Ru in some cases. This general statement has, however to be amended to account for observations in individual grains. One grain from Ingarinda (Fig. 8), as well as one grain and one aggregate from Burlakovsky (Fig. 7) imply the existence of preferred substitution of Os (\pm Ir) by Ru, but the trends defined by these grains are at variable Os/Ir ratios and are too small to be readily recognised.

Chemical zonation on the granular level reflect changes in conditions during the crystallisation of an individual Os-rich grain, while the change in bulk compositions of sets of grains give indications for the conditions of Os-rich grain formation on a larger scale. The overall trend of compositions in the Os-Ir-Ru system implies a systematic evolution of compositions as a result of the geochemical evolution throughout the Guli Massif.

Resampling statistics (Simon and Bruce 1991; Simon 1997) were used to evaluate to what degree the difference in average Ir-content of the grains from Ingarinda (mean = 17.49 at.%) and Burlakovsky (mean = 9.54 at.%) could be due to coincidence. For this purpose, subsets of values in the sizes of the two individual data sets were randomly

selected from the combined data set, the average calculated, and the difference between the averages evaluated. In 150,000 simulations it was not possible to even once create a difference larger than 80% of the difference observed in the real analyses, i.e., the error probability for a real difference between the populations is $\ll 0.0007$. The systematic difference in morphology and chemical composition of Os-rich alloy grains between the two sample populations at Ingaringda and Burlakovsky have also been noted in a companion study by Malitch et al. (2007). This variability supported by mineralogical evidence has been attributed to difference in rock sources.

Relationship of average composition with geological parameters

Any attempt to relate the composition of native osmium from placers to petrological characteristics of the source rocks can only be tentatively carried out. Obviously it is not possible to link placer PGM to specific rock types with any degree of certainty, because their source rocks had to be modified to permit release the PGM and to allow their concentration in placers.

It can only be expected that the chemical differences between populations of alloy grains (from different placers) follow the same pattern as on granular level (i.e., decreasing Os/Ir at relatively constant Ru) if it can be assumed that all grains of native osmium formed from the same type of melt. The observation of Ru-depletion trends (at approximately constant Os/Ir ratio, which could be explained by an increase in sulfur fugacity to the level that Ru-rich laurite formed and depleted the reservoir in Ru) and Ir-enrichment with only very low Ru contents (implies formation after substantial laurite formation) shows that additional factors may have been involved.

The Os/Ir values in rock samples (e.g., chromitite, dunite, and wehrlite) from the Guli Massif are between 2.4 and 2.8 (Malitch 1998). These values are indistinguishable within analytical uncertainties. A distinct difference exists for the Os/Ir value of magnetite clinopyroxenite (3.25). Native osmium with a composition similar to those of grains in the placers was found in dunite (Balmasova et al. 1992; Malitch et al. 2011) and chromitite (Malitch et al. 2003, 2011). Constant Os/Ir ratios imply that the melt(s) or residual rocks, from which these rocks originate, did not differ significantly in their ability to produce native osmium. This in turn makes it possible to assume that the observed zonation in native osmium grains, with increasing iridium contents towards the rim, represents the general sense of evolution within the Guli Massif. Consequently, native osmium with higher Ir contents should have formed after Ir-poor native osmium. This notion is described in some more detail (Malitch et al. 2011), suggesting that Os-rich alloy grains from chromitite are characterized by higher Ir contents (i.e. $\text{Os}_{66}\text{Ir}_{28}\text{Ru}_5$) compared to those in dunite ($\text{Os}_{84}\text{Ir}_{11}\text{Ru}_5$).

Our study demonstrated that the native osmium from Ingaringda has a systematically higher Ir tenor than grains from Burlakovsky. The grains from Ingaringda are therefore assumed to have either crystallized after those from Burlakovsky in a heterogeneous, deep-seated reservoir (from which they were extracted by different magma pulses), or they crystallized at a higher stratigraphic level in the Massif (if crystallization from the same silicate melt is assumed). That native osmium from Ingaringda is richer in Ru than that in Burlakovsky can

be explained by fluctuations in sulphur fugacity throughout the evolution of the Guli Massif or their crystallization in the Massif.

The trends with even higher Ir contents (Malitch et al. 2007, 2011) should then represent even further evolved parts of the Guli Massif or may point to distinct bedrock sources, like chromitites, more abundant in the upper parts of the Massif.

Although at present the Os/Ir ratio in native osmium can be tentatively linked to specific source rocks in the Guli massif, there is a need for further research to understand this relationship and to make more concrete predictions about the factors controlling the formation and mineral chemistry of native osmium.

Conclusions

The observations on native osmium from two placer occurrences in the Guli Massif lead to the following deductions:

- Compositional variations in native osmium from the Guli Massif differ significantly between the two studied placer localities.
- The agglomerated textures of Os-rich native osmium in aggregate nuggets from Burlakovsky, in which sub-grains differ strongly in composition, is considered unlikely to be possible under crustal conditions. It is concluded that they are inherited from the mantle source of the parental melt(s) of the Guli Massif.
- The nuggets from Ingarinda with less complex compositional variation in aggregates may have crystallised under crustal conditions from the evolving silicate melt(s).

Acknowledgements

We would like to express our gratitude towards Zeiss South Africa for assistance with microscope facilities and Wirsam Scientific for the loan of an ISIS system. Andre Botha's help to obtain the BSE images is highly appreciated. Constructive reviews by Prof. Andrew McDonald and Dr. Ibrahim Uysal are greatly appreciated. We express our gratitude to *Mineralogy and Petrology* Editor Johann G. Raith for his editorial input. This study was partly supported by Russian Foundation for Basic Research (grant 09-05-01242).

References

Ahmed HA (2007) Diversity of platinum-group minerals in podiform chromitites of the late Proterozoic ophiolite, Eastern Desert, Egypt: genetic implications. *Ore Geol Rev* 32:1–19

Arculus RJ (1994) Aspects of magma genesis in arcs. *Lithos* 33:189–208

Auge T, Johan Z (1988) Comparative study of chromite deposits from Troodos, Vourinos, North Oman and New Caledonia ophiolites. In: Boissonnas J and Omenetto P (eds) *Mineral deposits within the European Community*. Springer, Berlin, Heidelberg, Special Publication of the Society for Geology Applied to Mineral Deposits 6, pp. 267–288

Auge T, Legendre O, Maurizot P (1998) The distribution of Pt and Ru-Os-Ir minerals in the New Caledonia ophiolite. In: Laverov NP and Distler VV (eds) International Platinum. Theophrastus, St.-Petersburg, Athens, pp. 141–154

Balabonin NL, Korchagin AU, Latypov RM, Subbotin VV (1994) Fedorovo-Pansky Intrusion. In: Mitrofanov F and Torokhov M (editors) Kola belt of layered intrusions. Geological Institute Kola Science Centre, Russian Academy of Sciences, Apatity, 7th International Platinum Symposium. Guide to the pre-symposium field trip, pp. 9–41

Balmasova YA, Smol'skaya LS, Lopatina LA, Lopatin GG, Lazarenkov VG, Malitch KN (1992) Native osmium and iridosmine in the Gulinsky massif, Trans (Doklady) Russ Acad Sci / Earth Sci Sect 325:154–157 (translated from Dokl Rus Akad Nauk 323:748–751)

Barkov AY, Fleet ME, Nixon GT, Levson VM (2005) Platinum-group minerals from five placer deposits in British Columbia, Canada. *Can Mineral* 43:1687–1710

Betekhtin AG (1961) Mikroskopische Untersuchungen an Platinerzen aus dem Ural. *N Jahrb Mineral Abh* 97:1–34

Bird JM, Bassett WA (1980) Evidence of a deep mantle history in terrestrial osmium-iridium-ruthenium alloys. *J Geophys Res B Solid Earth Planets* 85:5461–5470

Bird JM, Meibom A, Frei R, Nagler TF (1999) Osmium and lead isotopes of rare OsIrRu minerals: derivation from the core-mantle boundary region? *Earth Planet Sci Lett* 170:83–92

Boehler R (1996) Melting temperature of the earth's mantle and core—earth's thermal structure. *Ann Rev Earth Planet Sci* 24:15–40

Brügmann GE, Reischmann T, Naldrett AJ, Sutcliffe RH (1997) Roots of an Archean volcanic arc complex: the Lac des Iles area in Ontario, Canada. *Precam Res* 81:223–239

Burg J-P, Bodinier J-L, Gerya T, Bedini R-M, Boudier F, Dautria J-M, Prihodko V, Efimov A, Pupier E, Balanec JL (2009) Translithospheric mantle diapirism: geological evidence and numerical modelling of the Kondyor zoned ultramafic Complex (Russian Far-East). *J Petrol* 50:289–321

Butakova EL (1974) Regional distribution and tectonic relations of the alkaline rocks of Siberia. In: Sorensen H (ed) *The alkaline rocks*, Chapter III, 4. John Wiley & Sons Ltd, London, pp 172–189

Cabri LJ (2002) The platinum-group minerals. In: Cabri J (ed) *The geology, geochemistry, mineralogy and mineral beneficiation of Platinum-group elements*. *Can Inst Mining Metall Petrol, Spec Vol* 54:13–129

Cabri LJ, Harris DC (1975) Zoning in Os-Ir alloys and the relation of the geological and the tectonic environment of the source rocks to the bulk Pt/(Pt+Ir+Os) ratio for placers. *Can Mineral* 13:266–274

- Cabri LJ, Laflamme JHG (1988) Mineralogical study of the platinum-group element distribution and associated minerals from three stratigraphic layers, Bird River Sill, Manitoba. CANMET, Energy, Mines and Resources Canada, Report CM 88-1E: 1–52
- LJ, Harris DC, Weiser TW (1996) Mineralogy and distribution of platinum-group mineral (PGM) placer deposits of the world. *Expl Mining Geol* 5:73–167
- Conrad WK, Kay RW (1984) Ultramafic and mafic intrusions from Adak Island: crystallization history and implications for the nature of primary magmas and crustal evolution in the Aleutian arc. *J Petrol* 25:88–125
- Cousins CA (1973) Platinoids in the Witwatersrand system. *J South Afri Instit Mining Metall* 73:184–199
- Dalrymple GB, Czamanske GK, Fedorenko VA, Simonov ON, Lanphere MA, Likhachev AP (1995) A reconnaissance $^{40}\text{Ar}/^{39}\text{Ar}$ study of ore-bearing and related rocks, Siberian Russia. *Geochim Cosmochim Acta* 59:2071–2083
- Dmitrenko GG, Mochalov AG, Palandzhyan SA, Goryacheva YM (1985) Chemical compositions of rock-forming and accessory minerals in Alpine-type ultramafites in the Koryak uplands. Part 2: Minerals of Platinum elements (in Russian). North–East Complex Research Institute of the Far East Centre of the Academy of Sciences, USSR, 128 pp
- Efimov AA (1998) The Platinum Belt of the Urals: structure, petrogenesis and correlation with platiniferous complexes of the Aldan Shield and Alaska. 8th International Platinum Symposium Abstracts. Geological Society of South Africa and the South African Institute of Mining and Metallurgy Symposium Series S18:93–96
- Egorov LS (1991) Ijolite-carbonatite plutonism (the Maimecha-Kotui Complex of Polar Siberia as an example). Nedra Press, Leningrad, 260 pp, in Russian
- El Ghorfi M, Melcher F, Oberthur T, Boukhari AE, Maacha L, Maddi A, Mhaili M (2008) Platinum-group minerals in podiform chromitites of the Bou Azzer ophiolite, Anti Atlas, Central Morocco. *Mineral Petrol* 92:59–80
- Feather CE (1976) Mineralogy of platinum-group minerals in the Witwatersrand, South Africa. *Econ Geol* 71:1399–1428
- Garuti G, Zaccarini F, Moloshag V, Alimov V (1999) Platinum-group minerals as indicators of sulfur fugacity in ophiolitic upper mantle: an example from chromitites of the Rai-Iz ultramafic complex, Polar Urals, Russia. *Can Mineral* 37:1099–1115
- Gonzalez-Jimenez JM, Gervilla F, Proenza JA, Auge T, Kerestedjian T (2010) Distribution of platinum-group minerals in ophiolitic chromitites. *Trans Institution Mining Metall, Sect B: Appl Earth Sci* 118:101–110
- Gornostayev SS, Crocket JH, Mochalov AG, Laajoki KVO (1999) The platinum-group minerals of the Baimka placer deposits, Aluchin horst, Russian Far East. *Can Mineral* 37:1117–1129

- Harris DC, Cabri LJ (1991) Nomenclature of platinum-group-element alloys: review and revision. *Can Mineral* 29:231–237
- Hattori K, Cabri LJ (1992) Origin of platinum-group-mineral nuggets inferred from an osmium-isotope study. *Can Mineral* 30:289–301
- Hiemstra SA (1964) Discussion of G.M. Koen's (1964) paper. *Trans Geol Soc South Afr* 67:288–290
- Kapsiotis A, Grammatikopoulos TA, Tsikouras B, Hatzipanagiotou K, Zaccarini F, Garuti G (2009) Chromian spinel composition and platinum-group element mineralogy of chromitites from the Milia area, Pindos ophiolite complex, Greece. *Can Mineral* 47:1037–1056
- Koen GM (1964) Rounded platinoid grains in the Witwatersrand blanket. *Trans Geol Soc South Afr* 67:139–147
- Kogarko LN, Zartman RE (2007) A Pb isotope investigation of the Guli massif, Maymecha-Kotuy alkaline-ultramafic complex, Siberian flood basalt province, Polar Siberia. *Mineral Petrol* 89:113–132
- Kogarko LN, Kononova VA, Orlova MP, Wooley AR (1995) Alkaline rocks and carbonatites of the world, part 2. Former USSR. Chapman and Hall, London, 226 pp
- Krstić S, Tarkian M (1997) Platinum-group minerals in gold-bearing placers associated with the Veluce ophiolite complex, Yugoslavia. *Can Mineral* 35:1–21
- Legendre O, Augé T (1986) Mineralogy of platinum-group mineral inclusions in chromites from different ophiolitic complexes. In: Gallagher MJ, Ixer RA, Neary CR, Prichard HM (eds) *Metallogeny of basic and ultrabasic rocks*. The Institution of Mining and Metallurgy, London, pp 361–372
- Malitch KN (1996) Platinoid placer of the Ingarinda River (north of the East Siberia). *Trans (Doklady) Russ Acad Sci / Earth Sci Sect* 349:723–727 (translated from *Dokl Akad Nauk* 348:652–656)
- Malitch KN (1998) Peculiarities of platinum-group element distribution in ultramafites of clinopyroxenite-dunite massifs as an indicator of their origin. In: Laverov NP and Distler VV (eds) *International Platinum, Theophrastus Publ, St.-Petersburg, Athens*, pp. 129–140.
- Malitch KN (1999) Platinum-group elements in clinopyroxenite-dunite massifs of the Eastern Siberia (geochemistry, mineralogy, and genesis). St. Petersburg Cartographic Factory VSEGEI Press, St. Petersburg, 296 pp, in Russian
- Malitch KN, Kostoyanov AI (1999) Model Re-Os isotopic age of the PGE mineralization at the Gulinsk Massif (at the Northern Siberian Platform, Russia). *Geol Ore Deposits* 41:126–135

Malitch KN, Lopatin GG (1997a) Geology and petrographic association of ultramafites of the Guli intrusion. In: Simonov ON, Malitch NS (eds) Nedra Taimyra (Resources of Taimyr) vol 2. VSEGEI Press, Noril'sk – St.Petersburg, pp 86–103, in Russian

Malitch KN, Lopatin GG (1997b) New data on the metallogeny of the unique Guli clinopyroxenite-dunite massif (Northern Siberia, Russia). *Geol Ore Deposits* 39:209–218

Malitch KN, Merkle RKW (2004) Ru-Os-Ir-Pt and Pt-Fe alloys from the Evander Goldfield (Witwatersrand Basin, South Africa): detrital origin inferred from compositional and osmium isotope data. *Can Mineral* 42:631–650

Malitch KN, Rudashevsky NS (1994) Bedrock platinum-metal mineralization in chromitite of the Guli massif. *Trans (Dokl) Russ Acad Sci Earth Sci Sect* 327(8):165–169

Malitch KN, Badanina IY, Goncharov MM, Lopatin GG, Naumenko NG, Tuganova EV (1996) The Maimecha-Kotui region—a new platinum province in Russia. *Trans (Doklady) Russ Acad Sci / Earth Sci Sect* 348:574–577 (translated from *Dokl Akad Nauk* 348:232–235)

Malitch KN, Malitch NS, Simonov ON, Lopatin GG, Naumenko NG (1998) New unique osmium source in Russia. 8th Int. Platinum Symposium Abstracts. Geological Society of South Africa and the South African Institute of Mining and Metallurgy Symposium Series S18, pp. 235–238

Malitch KN, Auge T, Badanina IYu, Goncharov MM, Junk SA, Pernicka E (2002) Os-rich nuggets from Au-PGE placers of the Maimecha-Kotui Province, Russia: a multi-disciplinary study. *Mineral Petrol* 76:121–148

Malitch KN, Zaccarini F, Garuti G (2003) Preliminary results of the “in situ” investigation of platinum-group minerals in chromitites from the Kondyor and Guli ultramafic massifs (Russia). In: Eliopoulos DG et al (eds) *Mineral exploration and sustainable development*. Millpress, Rotterdam, pp. 611–614

Malitch KN, Knauf VV, Meisel T, Paliulionyte V, Efimov AA, Kostoyanov AI (2005) Contrasting platinum-group mineral assemblages from chromitites of clinopyroxenite-dunite massifs (Russia): new compositional and osmium isotope data. In: Tormanen TO, Alapieti TT (eds) *10th International Platinum Symposium, Extended abstracts*, Espoo, Geological Survey of Finland, pp. 186–189

Malitch KN, Badanina IYu, Kapitonov IN, Junk SA (2007) A combined SEM, EMPA and LA MC ICP-MS study of Os-rich alloys from the Guli Massif, Maimecha-Kotui Province, Russia: new data. In: Andrew CJ et al. (eds) *Digging deeper. Proceedings of the Ninth Biennial Meeting of the Society for Geology Applied to Mineral Deposits vol 2*, Ireland, Cambridge Mineral Resources plc., pp. 1583–1586

KN, Kadik AA, Badanina IYu, Zharkova EV (2011) Redox conditions of formation of osmium-rich minerals from the Guli Massif, Russia. *Geochem Intern* 49:726–730

Massalski TB (editor) (1993) Binary alloy phase diagrams. Am Soc Metals, Metals Park, Ohio, 2224 pp

McKelson JF, Thalhammer OAR, Paliulionyte V (2005) The dunite complex of the Guli massif, northern Siberia, Russia: a multidisciplinary study. *Mitt Österr Mineral Ges* 15:91–95

Melcher F (2000) Chromite and platinum-group elements as indicators of mantle petrogenesis. Habilitation thesis, Montanuniversitaet Leoben, Austria

Melcher F, Grum W, Simon G, Thalhammer TV, Stumpfl EF (1997) Petrogenesis of the ophiolitic giant chromite deposits of Kempirsai, Kazakhstan: a study of solid and fluid inclusions in chromite. *J Petrol* 38:1419–1458

Merkle RKW (1998) Proportions of magmatic platinum-group minerals and evolution of mineralizing processes, UG-1 chromitite layer, Bushveld Complex. In: Laverov NP, Distler VV (eds) *International Platinum. Theophrastus, St.-Petersburg, Athens*: pp. 43–53

Merkle RKW, Franklin CB (1999) Milli-PIXE determinations of trace elements in osmium-rich platinum-group minerals from the Witwatersrand Basin, South Africa. *Nucl Instr Meth Phys Res B* 158:556–561

Mues-Schumacher U, Keller J, Kononova VA, Suddaby PJ (1996) Mineral chemistry and geochronology of the potassic alkaline ultramafic Inagli Complex, Aldan Shield, Eastern Siberia. *Mineral Mag* 60:711–730

Murray CG (1972) Zoned ultramafic complexes of the Alaskan type: feeder pipes of andesitic volcanoes. *Geol Soc Am Mem* 132:313–335

Nakagawa M, Franko HA (1997) Placer Os-Ir-Ru alloys and sulfides: indicators of sulfur fugacity in an ophiolite. *Can Mineral* 35:1441–1452

Ohnenstetter M (1992) Platinum group element enrichment in the upper mantle peridotites of the Monte Maggiore ophiolitic massif (Corsica, France): mineralogical evidence for ore-fluid metasomatism. *Mineral Petrol* 46:85–107

Ohnenstetter M, Karaj N, Neziraj A, Johan Z, Cina A (1991) Platiniferous potential of ophiolites: PGE mineralizations in the ophiolitic complexes of Tropoja and Bulqiza, Albania. *Compt Rend Acad Sci Ser II* 313:201–208 (in French)

Okrugin AV (2002) Phase transformations and genesis of platinum-group minerals in various types of platinum-bearing deposits. In 9th International Platinum Symposium (Billings), In Boudreau AE (ed), *Extended Abstracts*, Duke University Press, Durham, North Carolina, pp. 349–353

Peacock SM, Rushmer T, Thompson AB (1994) Partial melting of subducting oceanic crust. *Earth Planet Sci Lett* 121:227–244

Peck DC, Keays RR, Ford RJ (1992) Direct crystallization of refractory platinum-group element alloys from boninitic magmas: evidence from western Tasmania. *Austral J Earth Sci* 39:373–387

Rozhkov IS, Kitsul VI, Razin LV, Borishanskaya SS (1962) Platinum of Aldan shield. Academy of Sciences of the USSR, Moscow, p 162, in Russian

Schmidt MW, Poli S (1998) Experimentally based water budgets for dehydrating slabs and consequences for arc magma generation. *Earth Planet Sci Lett* 163:361–379

Sherman DM (1997) The composition of the Earth's core: constraints on S and Si vs. temperature. *Earth Planet Sci Lett* 153:149–155

Shi R, Alard O, Zhi X, O'Reilly SY, Pearson NJ, Griffin WL, Zhang M, Chen X (2007) Multiple events in the Neo-Tethyan oceanic upper mantle: evidence from Ru-Os-Ir alloys in the Luobusa and Dongqiao ophiolitic podiform chromitites, Tibet. *Earth Planet Sci Lett* 261:33–48

Simon JL (1997) *Resampling: The "New Statistics"*, 2nd edn. Resampling Stats Inc, Arlington, 436

Simon JL, Bruce P (1991) Resampling: a tool for everyday statistical work. *Chance* 4:22–32

Sobolev AV, Sobolev SV, Kuzmin DV, Malitch KN, Petrunin AG (2009) Siberian meimechites: origin and relation to flood basalts and kimberlites. *Russ Geol Geophys* 50:999–1033

St. Louis RM, Nesbitt BE, Morton RD (1986) Geochemistry of platinum-group elements in the Tulameen ultramafic complex, southern British Columbia. *Econ Geol* 81:961–973

Tolstykh ND, Sidorov EG, Krivenko AP (2005) Platinum-group element placers associated with Ural-Alaska type complexes. In: Mungall JE (ed). *Exploration for platinum-group element deposits*. Min Ass Can Short Course Ser 35:113–143

Tolstykh N, Sidorov E, Kozlov A (2009) Platinum-group minerals from the Olkhovaya-1 placers related to the Karaginsky ophiolite complex, Kamchatskiy Mys Peninsula, Russia. *Can Mineral* 47:1057–1074

Uysal I, Tarkian M, Sadiklar MB, Zaccarini F, Meisel T, Garuti G, Heidrich S (2009) Petrology of Al- and Cr-rich ophiolitic chromitites from the Muğla, SW Turkey: implications from composition of chromite, solid inclusions of platinum-group mineral, silicate, and base-metal mineral, and Os-isotope geochemistry. *Contrib Mineral Petrol* 158:659–674

Vasil'ev YuR, Zolotukhin VV (1975) Petrology of the ultramafites in the North of the Siberian Platform and some problems of their genesis. Nauka Press, Novosibirsk, p 271, in Russian

Vasil'ev YuR, Zolotukhin VV (1995) The Maimecha-Kotui alkaline-ultramafic province of the northern Siberian platform, Russia. *Episodes* 18:155–164

Weiser TW (2002) Platinum-group minerals (PGM) in placer deposits. In: Cabri LJ (ed.) The geology, geochemistry, mineralogy and mineral beneficiation of Platinum-group elements. *Can Inst Mining Metallu Petrol Spec* 54:721–756

Weiser TW, Bachmann HG (1999) Platinum-group minerals from the Aikora River area, Papua New Guinea. *Can Mineral* 37:1131–1145

Zaccarini F, Proenza JA, Ortega-Gutiérrez F, Garuti G (2005) Platinum group minerals in ophiolitic chromitites from Tehuizingo (Acatlán complex, southern Mexico): Implications for post-magmatic modification. *Mineral Petrol* 84:147–168

Zhabin AG (1965) Structure and succession formation of the Guli dunite complex, ultramafic and ultramafic-alkaline lavas, alkaline rocks and carbonatites. In: Borodin LS (ed) *Petrology and geochemical features of ultramafic and alkaline rock associations and carbonatites*. Nauka Press, Moscow, pp 160–192 (in Russian)